Global ab initio potential energy surfaces for the O 2 (3 g) + O 2 (3 g) interaction

Massimiliano Bartolomei, Estela Carmona-Novillo, Marta I. Hernández, José Campos-Martínez, and Ramón Hernández-Lamoneda

Citation: The Journal of Chemical Physics **133**, 124311 (2010); doi: 10.1063/1.3479395
View online: http://dx.doi.org/10.1063/1.3479395
View Table of Contents: http://scitation.aip.org/content/aip/journal/jcp/133/12?ver=pdfcov
Published by the AIP Publishing

Global *ab initio* potential energy surfaces for the $O_2(^3\Sigma_g^-)+O_2(^3\Sigma_g^-)$ interaction

Massimiliano Bartolomei,[1,a)] Estela Carmona-Novillo,[1] Marta I. Hernández,[1] José Campos-Martínez,[1] and Ramón Hernández-Lamoneda[2]
[1]*Instituto de Física Fundamental, Consejo Superior de Investigaciones Científicas, Serrano 123, 28006 Madrid, Spain*
[2]*Centro de Investigaciones Químicas, Universidad Autónoma del Estado de Morelos, 62210 Cuernavaca, Morelos, Mexico*

(Received 8 June 2010; accepted 23 July 2010; published online 24 September 2010)

Completely *ab initio* global potential energy surfaces (PESs) for the singlet and triplet spin multiplicities of rigid $O_2(^3\Sigma_g^-)+O_2(^3\Sigma_g^-)$ are reported for the first time. They have been obtained by combining an accurate restricted coupled cluster theory with singles, doubles, and perturbative triple excitations [RCCSD(T)] quintet potential [Bartolomei *et al.*,J. Chem. Phys. **128**, 214304 (2008)] with complete active space second order perturbation theory (CASPT2) or, alternatively, multireference configuration interaction (MRCI) calculations of the singlet-quintet and triplet-quintet splittings. Spherical harmonic expansions, containing a large number of terms due to the high anisotropy of the interaction, have been built from the *ab initio* data. The radial coefficients of these expansions are matched at long range distances with analytical functions based on recent *ab initio* calculations of the electric properties of the monomers [M. Bartolomei, E. Carmona-Novillo, M. I. Hernández, J. Campos-Martínez, and R. Hernández-Lamoneda, J. Comput. Chem. (2010) (in press)]. The singlet and triplet PESs obtained from either RCCSD(T)-CASPT2 or RCCSD(T)-MRCI calculations are quite similar, although quantitative differences appear in specific terms of the expansion. CASPT2 calculations are the ones giving rise to larger splittings and more attractive interactions, particularly in the region of the absolute minima (in the rectangular D_{2h} geometry). The new singlet, triplet, and quintet PESs are tested against second virial coefficient B(T) data and, their spherically averaged components, against integral cross sections measured with rotationally hot effusive beams. Both types of multiconfigurational approaches provide quite similar results, which, in turn, are in good agreement with the measurements. It is found that discrepancies with the experiments could be removed if the PESs were slightly more attractive. In this regard, the most attractive RCCSD(T)-CASPT2 PESs perform slightly better than the RCCSD(T)-MRCI counterpart. © *2010 American Institute of Physics*. [doi:10.1063/1.3479395]

I. INTRODUCTION

The calculation of global potential energy surfaces (PES) represents a crucial step for analyzing and predicting a wide range of molecular properties. A great deal of effort has been applied in this direction specially in the recent past motivated by the development of powerful electronic structure methods[1] and the ever increasing improvements in computational resources. Still, most of the systems studied so far belong to the closed shell category, and much less has been accomplished for the more challenging open-shell cases. In this regard, it is worth mentioning that several groups are still actively pursuing the development of new methodologies.[2–9] One of the most difficult cases for the current state of the art *ab initio* methodologies is the interaction of two open-shell monomers[10] where the most accurate and well-established single reference methods fail completely. In order to tackle such problems, one has to rely on multiconfigurational methods and deal with their limitations when applied to weakly interacting systems.

A prototypical tetratomic system with two open-shells is $[O_2(^3\Sigma_g^-)]_2$, which leads to asymptotically degenerate singlet, triplet, and quintet states. In a pioneering work,[11,12] global PESs for the three multiplicities were built on the basis of first order exchange intermolecular perturbation theory and subsequently used to study properties of the solid phases.[13] Some years later, Bussery and Wormer (BW) (Ref. 14) added empirical dispersion coefficients in order to obtain a more realistic description by including the most important attractive terms. Molecular beam experiments by the Perugia group[15,16] led to global PES for the different multiplicities via an inversion procedure of their extensive cross section data. At the same time, new high resolution spectra were recorded,[17,18] showing a high degree of congestion and complicating its analysis, and for this purpose, the use of the BW PES was crucial. More recently, interest in the molecular oxygen dimer has come from the rapidly expanding field of cold and ultracold collisions, where the system has been considered as a likely candidate for evaporative cooling[19] and quantum scattering calculations have been performed using both the BW PES (Ref. 20) and the Perugia PES.[21,22] Finally, the relevance of oxygen complexes for absorption processes

a)Electronic mail: maxbart@iff.csic.es.

in the atmosphere[23,24] including its possible interference with the Chappuis and Hartley bands of ozone[25] is well recognized and documented.

Although both BW and Perugia PESs have been of great importance in interpreting the available experimental data and have been shown to be consistent with reliable *ab initio* calculations,[26–28] there are significant discrepancies between them reflecting their inherent limitations. This together with the wealth of detailed experimental information available has prompted us to develop highly accurate global *ab initio* PESs. In a previous paper,[29] we presented a PES for the quintet state calculated with the restricted coupled cluster theory with singles, doubles, and perturbative triple excitations method [RCCSD(T)] and an extensive basis. We predicted the presence of a new local minimum skewed structure, indicating the power of the methodology followed. Additionally the PES has been used in scattering calculations,[30] and a critical comparison with the Perugia potential has been made. As mentioned above, *ab initio* calculations of the singlet and triplet states are much more difficult. In Ref. 26, we proposed that the singlet and triplet potentials can be adequately obtained by combining RCCSD(T) quintet potentials with multireference configuration interaction (MRCI) calculations of the singlet-quintet and triplet-quintet splittings. A more detailed analysis at the four limiting geometrical arrangements of the dimer was performed later[31] by comparing several multiconfigurational approaches such as MRCI, averaged coupled-pair functional, and complete active space second order perturbation theory (CASPT2) for different active spaces and basis sets. This study allowed us to test the influence of improving the size consistency error, which is a delicate point when treating weak intermolecular forces. We were also able to conclude on the limitations of the Heisenberg Hamiltonian, which has been used so frequently in the past to treat this type of interaction and the need to include higher order correlation to accurately describe the splittings between the multiplet states. Finally, we showed that calculations of the splittings with the MRCI and CASPT2 methods should provide lower and upper limits, respectively, to the interaction. The aim of the present work is to extend these calculations to construct fully *ab initio* global PESs for the singlet and triplet states.

In Sec. II, we provide details for the building of the *ab initio* global PESs and how the supermolecular calculations are matched in the long range region with analytical functions with coefficients obtained from *ab initio* calculations of monomer properties.[32] Section III is devoted to the analysis of the potential energy surfaces, the comparison with measured total cross sections,[16] and second virial coefficient data.[33,34] Comparisons with the experimentally derived Perugia PES (Ref. 16) will be also discussed in this section. Concluding remarks are finally given in Sec. IV.

II. CALCULATION OF SINGLET AND TRIPLET POTENTIAL ENERGY SURFACES

Following Ref. 31, the singlet (s) and triplet (t) interaction energies are obtained by adding, to the RCCSD(T) quintet (q) potential,[29] V^q_{CC}, singlet-quintet ($s-q$) and triplet-quintet ($t-q$) splittings computed using a multiconfigurational method,

$$V^s_{\mathrm{CC-multi}} = V^q_{\mathrm{CC}} + \Delta^{s-q}_{\mathrm{multi}},$$
$$V^t_{\mathrm{CC-multi}} = V^q_{\mathrm{CC}} + \Delta^{t-q}_{\mathrm{multi}}, \tag{1}$$

$$\Delta^{s,t-q}_{\mathrm{multi}} = V^{s,t}_{\mathrm{multi}} - V^q_{\mathrm{multi}}, \tag{2}$$

where $V^{s,t,q}_{\mathrm{multi}}$ are $S=0,1,2$ state energies as obtained by a *multi*configurational method and S is the total electronic spin. A similar approach has been recently adopted for the study of the $[\mathrm{NH}(^3\Sigma^-)]_2$ dimer.[35,36] Here, the $s-q$ and $t-q$ splittings are computed at MRCI as well as CASPT2 levels of theory based on previous findings from Ref. 31. In this way, we have built *two* types of singlet and triplet PESs, referred in what follows as CC-MRCI and CC-PT2 PESs, where "CC" refers to the RCCSD(T) calculation of the quintet state, and the second acronym refers to the method used to compute the splittings, MRCI and CASPT2, respectively.

A. Geometries and *ab initio* calculations

We have considered different relative geometries of the dimer based in diatom-diatom Jacobi coordinates: the intermolecular distance R, the angles θ_a and θ_b, formed between the intermolecular $\mathbf{R}$ and the intramolecular vectors $\mathbf{r_a}$, and $\mathbf{r_b}$, respectively, and the torsional angle ϕ. In all the calculations, r_a and r_b distances have been fixed to the O_2 equilibrium distance, $r_e=2.28$ bohrs (rigid monomers). For the intermolecular distance R, 18 values ranging from 4.5 to 16.0 bohrs were considered. For the angular variables, we have taken the geometries coming out from nine Gauss–Legendre quadrature points in the $-1\leq\cos\theta_a,\ \cos\theta_b\leq 1$ range and from five Gauss–Chebyshev quadrature points for $0\leq\phi\leq\pi$. Several of the resulting geometries are equivalent due to the symmetry of the system, and the ranges of the coordinates have been reduced to 65 "irreducible geometries," as described in Ref. 29. We thus have computed 1170 points for each spin state ($S=0,1,2$) and multiconfigurational (MRCI and CASPT2) approach.

The applied *ab initio* methodology has been guided by our previous detailed study[31] on the performance of several multireference approaches for the calculation of the multiplet splittings in the system. In that study, several tests were made regarding the choice of the active space, a crucial ingredient of the multireference methods and also on the choice of one electron basis set. We selected the active space consisting of distributing 12 electrons in eight active molecular orbitals correlating with the molecular oxygen π shell. As mentioned before dynamical correlation effects are treated at the MRCI and CASPT2 levels since they provide, respectively, lower and upper limits to the interaction energy. The 5s4p3d2f atomic natural orbital basis set[37] plus the bond function set [3s3p2d1f] developed by Tao[38] placed in the middle of the complex has been used. This choice of basis set and active space is a good compromise between accuracy and computational expediency.

TABLE I. Comparison of *ab initio* energies (V_{abi}) with energies resulting from the spherical harmonic expansion of Eq. (3) (V_{fit}) using the set of 27 and 29 radial terms for the CC-PT2 and CC-MRCI PESs, respectively, for several orientations and intermolecular distances.

		Singlet				Triplet			
		CC-PT2		CC-MRCI		CC-PT2		CC-MRCI	
Geometry	R (bohr)	V_{abi} (meV)	V_{fit} (meV)	V_{abi} (meV)	V_{fit} (meV)	V_{abi} (meV)	V_{fit} (meV)	V_{abi} (meV)	V_{fit} (meV)
H ($\theta_a=\pi/2$, $\theta_b=\pi/2$, and $\phi=0$)	5.00	−18.44	−20.05	0.58	4.86	22.41	18.75	37.16	31.02
	5.50	−32.13	−32.79	−23.46	−23.08	−15.95	−16.70	−9.63	−10.41
	6.00	−28.46	−28.62	−24.50	−24.45	−22.15	−22.27	−19.36	−19.42
	7.00	−14.61	−14.63	−13.81	−13.81	−13.64	−13.64	−13.09	−13.10
	9.00	−3.16	−3.16	−3.12	−3.13	−3.13	−3.13	−3.10	−3.11
X ($\theta_a=\pi/2$, $\theta_b=\pi/2$, and $\phi=\pi/2$)	5.00	58.91	56.51	63.10	54.89	59.01	64.36	61.95	72.09
	5.50	−2.50	−2.37	0.15	−0.34	−2.01	−0.99	−0.17	0.67
	6.00	−16.66	−16.57	−15.14	−15.15	−16.24	−16.08	−15.19	−15.10
	7.00	−12.53	−12.52	−12.13	−12.12	−12.38	−12.37	−12.12	−12.10
	9.00	−3.04	−3.04	−3.02	−3.02	−3.03	−3.03	−3.01	−3.02
T ($\theta_a=\pi/2$ and $\theta_b=0$)	5.00	541.34	537.74	570.00	564.86	601.97	607.73	627.05	628.70
	5.50	154.81	153.92	168.40	167.82	183.18	183.47	193.71	193.77
	6.00	24.90	24.79	30.98	31.05	36.23	36.28	40.63	40.74
	7.00	−17.19	−17.20	−15.98	−15.94	−15.48	−15.49	−14.65	−14.64
	9.00	−5.15	−5.15	−5.14	−5.12	−5.11	−5.11	−5.11	−5.09
L ($\theta_s=0$ and $\theta_b=0$)	5.50	1758.66	1759.47	1795.15	1800.14	1980.83	1979.68	2016.94	2015.87
	6.00	584.51	585.69	603.96	605.80	646.49	646.93	660.81	661.35
	7.00	26.84	27.05	30.02	30.30	33.54	33.66	35.76	35.89
	9.00	−9.05	−9.06	−8.93	−8.95	−8.91	−8.93	−8.83	−8.86

The counterpoise method[39,40] was applied in order to correct the interaction energies for the basis set superposition error. In addition, Davidson's correction[41,42] was added to the MRCI energies. For both MRCI and CASPT2 calculations, the residual interaction energy calculated at the asymptote ($R=70$ bohrs), which arises from the size consistency error, is subtracted at all calculated points. It should be noted that this error is about one order of magnitude smaller in the case of CASPT2 (about 50 meV) as compared with MRCI. For a detailed analysis of the size consistency error in multireference second order perturbation theory, see Ref. 43. In the case of the quintet surface, a very small residual due to the approximate spin adaptation in RCCSD(T) (Ref. 44) also has to be subtracted. In particular, the size consistency error is about 0.1 meV for our present RCCSD(T) calculations and reduces to about 0.001 meV when spin-unrestricted CCSD(T) [UCCSD(T)] is employed. These numbers are similar to those reported in Ref. 36, where the authors compared both methods and found that subtracting the size consistency error for the RCCSD(T) energies does not significantly change the accuracy of the potential but does give the desired asymptotic behavior at long range. On the other hand, the use of the restricted formalism guarantees conservation of spin, which is very important for this system. Finally, for the CASPT2 calculations, the standard RS2 program of MOLPRO (Ref. 45) has been used since, compared with the RS2C version, it provided more stable and reliable results. All calculations have been performed with the MOLPRO 2002.3 package.[45]

B. Spherical harmonics expansion

The interaction potentials $V^{s,t}_{CC-multi}$ are expressed by means of the spherical harmonics expansion,[12]

$$V^{s,t}_{CC-multi}(R,\theta_a,\theta_b,\phi) = (4\pi)^{3/2}\sum_{l_a,l_b,l} f^{l_a l_b l}_{s,t}(R) A_{l_a l_b l}(\theta_a,\theta_b,\phi), \quad (3)$$

with

$$A_{l_a l_b l}(\theta_a,\theta_b,\phi) = \left(\frac{2l+1}{4\pi}\right)^{1/2}\sum_m \begin{pmatrix} l_a & l_b & l \\ m & -m & 0 \end{pmatrix} Y_{l_a,m}(\theta_a,0) Y_{l_b,-m}(\theta_b,\phi), \quad (4)$$

where $Y_{l_a,m}$ and $Y_{l_b,-m}$ are spherical harmonics coupled by a $3-j$ symbol, l_a, l_b, and l are even integers (due to symmetry), and m runs from $-\min(l_a,l_b)$ to $\min(l_a,l_b)$. The radial coefficients $f^{l_a l_b l}_{s,t}(R)$ are obtained by integrating $V^{s,t}_{CC-multi}$ over the angular variables by means of Gauss–Legendre and Gauss–Chebyshev quadratures on the grid of angular orientations defined above.[29]

After a careful analysis of the radial coefficients that can be obtained from the present set of quadrature points, we have found that for the CC-MRCI PESs, the set of $(l_a l_b l)$ labels previously used for the quintet RCCSD(T) PES (Ref. 29) was adequate (the complete list of terms can be seen in Table II). For the CC-PT2 PESs, it was found that an expansion using 27 terms, where the $(l_a l_b l)=(8\ 2\ 8)$ and $(8\ 4\ 4)$ terms are taken out from the above set, was better suited to represent the interaction. We have computed the root mean square relative errors of the expansions with respect to the *ab initio* energies, averaged over all distances and quadrature points, obtaining 2% and 5% for the CC-PT2 and CC-MRCI PESs, respectively. A further indication of the quality of the expansion is given in Table I, where the spherical harmonic

TABLE II. Radial coefficients, $f^{l_a l_b l}$, of the spherical harmonic expansion for the singlet CC-PT2 and CC-MRCI PESs (in meV) at $R=6$ bohr and triplet-singlet ($t-s$) splittings, $f_t^{l_a l_b l}-f_s^{l_a l_b l}$, at the same distance. Note that RCCSD(T) calculations are not involved in the splittings [see Eq. (2)] and, also, that the $(l_a l_b l)=(8\ 2\ 8)$ and (8 4 4) terms are not included in the CC-PT2 expansion. Items within parentheses indicate that the absolute value of the corresponding radial terms is $<10^{-2}$ meV.

			Singlet		$t-s$ splitting	
l_a	l_b	l	CC-PT2	CC-MRCI	CASPT2	MRCI
0	0	0	53.36	56.82	5.70	4.89
2	0	2	56.84	57.74	2.67	2.53
2	2	0	10.48	10.66	0.57	0.54
2	2	2	−17.54	−17.59	−0.31	−0.34
2	2	4	38.51	38.92	1.55	1.49
4	0	4	8.54	8.46	−0.65	−0.68
4	2	2	1.65	1.62	−0.12	−0.12
4	2	4	−2.01	−2.06	0.01	0.02
4	2	6	7.59	7.32	−0.74	−0.69
4	4	0	−0.02	−0.02	0.05	0.05
4	4	2	−0.07	−0.05	−0.01	−0.02
4	4	4	(<.01)	−0.01	0.03	0.03
4	4	6	0.25	0.25	−0.15	−0.17
4	4	8	−6.49	−5.31	3.70	3.37
6	0	6	0.78	0.76	−0.25	−0.26
6	2	4	0.18	0.17	−0.03	−0.03
6	2	6	−0.21	−0.22	0.06	0.06
6	2	8	0.94	0.83	−0.28	−0.27
6	4	6	0.02	0.02	−0.03	−0.03
6	4	8	0.09	0.10	0.01	(<.01)
6	4	10	−2.71	−2.32	1.40	1.29
6	6	12	−1.46	−1.27	0.83	0.78
8	0	8	0.08	0.08	−0.04	−0.04
8	2	8	⋯	−0.03	⋯	0.01
8	2	10	0.13	0.11	−0.05	−0.05
8	4	4	⋯	0.04	⋯	−0.03
8	4	12	−0.50	−0.43	0.30	0.27
8	6	14	−0.36	−0.32	0.26	0.24
8	8	16	−0.12	−0.10	0.05	0.05

expansions are compared with the *ab initio* calculations performed at specific dimer orientations. Note that except for the X geometry, these points do not belong to the set originally considered for building the PESs. In addition, a comparison corresponding to the singlet state is displayed in Fig. 1. It can be seen that the spherical harmonic expansions used here are quite accurate. The largest discrepancies are found at short intermolecular distances ($R \leq 5$ bohrs), where the interaction is highly anisotropic.

C. Long range behavior and matching procedure

At large intermolecular distances, exchange effects are negligible, and hence the singlet, triplet, and quintet interaction potentials become degenerate. In this subsection, we present the asymptotic extension of the singlet, triplet, and quintet[29] PESs using a common analytical long range behavior.

Within the perturbation theory framework, the radial coefficients $f^{l_a l_b l}(R)$ of Eq. (3) can be written by a sum of electrostatic, dispersion, and induction contributions denoted by the subscripts *el*, *d*, and *i*, respectively,

$$f^{l_a l_b l}(R) = f_{el}^{l_a l_b l}(R) + f_d^{l_a l_b l}(R) + f_i^{l_a l_b l}(R), \tag{5}$$

with

$$f_{el}^{l_a l_b l}(R) = \delta_{l_a+l_b,l}\left[\frac{(2l_a+2l_b)!}{(2l_a+1)!(2l_b+1)!}\right]^{1/2}\frac{Q_0^{l_a}Q_0^{l_b}}{R^{l_a+l_b+1}} \tag{6}$$

and

$$f_{(d,i)}^{l_a l_b l}(R) = -\frac{1}{[(2l_a+1)(2l_b+1)(2l+1)]^{1/2}}\sum_n \frac{C_{n,(d,i)}^{l_a l_b l}}{R^n}. \tag{7}$$

Long range coefficients for O_2+O_2 have been recently obtained in our group by means of high level *ab initio* calculations.[32] Permanent electric multipole moments Q_0^l ($l=2,4,6,8$) were taken from Table III in Ref. 32 and dispersion and induction coefficients $C_{n,(d,i)}^{l_a l_b l}$ [with $n=6,8$ and $n=8$, respectively, and $(l_a l_b l)$ up to (4 2 6)] from Table V of the same work.

The matching between the radial coefficients obtained from the supermolecular *ab initio* calculations and the long range expansion has been performed as follows. For each term $(l_a l_b l)$, an additional point R_{N+1} at 19 bohrs was in-

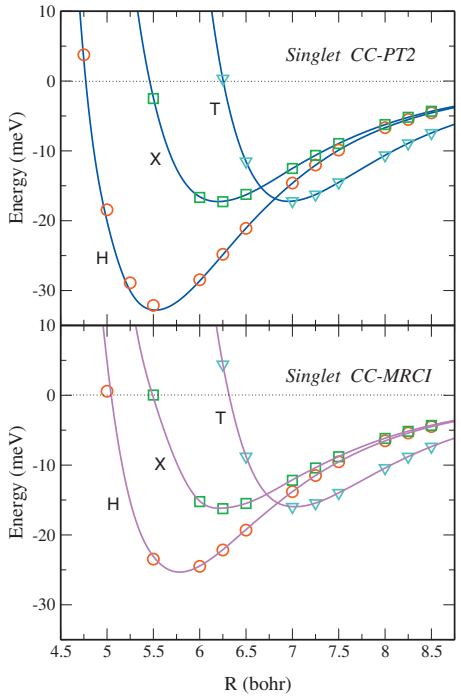

FIG. 1. Comparison between the spherical harmonic expansion of Eq. (3) (lines) with *ab initio* calculations (points) for the singlet CC-PT2 and CC-MRCI PESs at the limiting orientations H ($\theta_a=\theta_b=\pi/2, \phi=0$), X ($\theta_a=\theta_b=\phi=\pi/2$), and T ($\theta_a=\pi/2, \theta_b=0$).

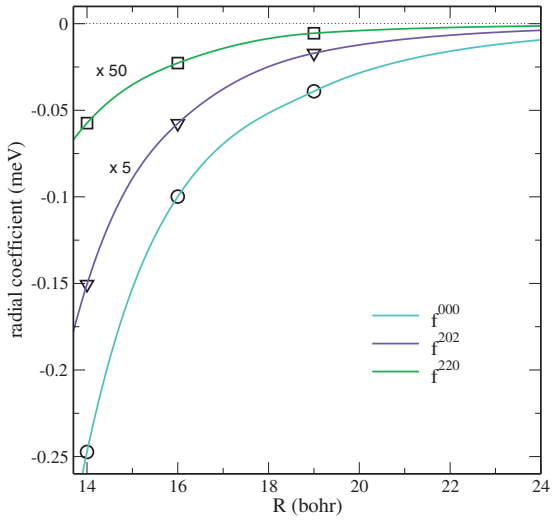

FIG. 2. Behavior of the f^{000}, f^{202}, and f^{220} radial coefficients of the triplet CC-PT2 PES at large intermolecular distances. Points at 14 and 16 bohrs are those resulting from the *ab initio* calculations, whereas the point at 19 bohrs is given by Eq. (5). The curves are, for $R<19$ bohrs, the result of cubic spline interpolation, while for larger R's, they are given by the analytical long range behavior of Eq. (5). See text for more details.

cluded in the grid of intermolecular distances and assigned the value given by Eq. (5). For distances between R_1 and R_{N+1}, the energy of the term is obtained by cubic spline interpolation. The analytical derivative of $f^{l_a l_b l}(R)$ at R_{N+1} was used as a boundary condition for solving the interpolation equations in order to obtain a smooth behavior of the term around R_{N+1}. The analytical behavior is then used for distances larger than R_{N+1}. For those terms with unknown long range behavior (12 terms), an adequate exponential decay was imposed for the asymptotic behavior.

The procedure worked quite well for the quintet PES,[29] and especially well for those coefficients dominating the spherical harmonic expansion. This is a good indication of the consistency between the supermolecular calculations and the calculations of the electric properties of the molecular fragments. For the singlet and triplet PESs, we have found some difficulties: the computed splittings $\Delta^{s,t-q}_{\text{multi}}$ [Eq. (2)] typically display an exponential-like decay at intermediate distances, but after reaching values of the order of 10^{-2} meV at about 10 bohrs, they do not continue rapidly decreasing to zero for larger R's but keep values between 10^{-3} and 10^{-2} meV. These inaccuracies are unimportant for the long range behavior of the isotropic terms but become relevant for the appropriate matching of the anisotropy terms of the expansion. The problem has been corrected by adjusting the splittings with suitable exponentially decreasing functions for distances larger than 10 bohrs. After this, all singlet and triplet curves become almost coincident with the quintet RCCSD(T) ones for large distances ($R>14$ bohrs), and the matching with the long range expansion is as smooth as that of the quintet PES. As an example of the quality of the fit, we show in Fig. 2 the matching of the first three terms of the spherical harmonic expansion for the case of the triplet CC-PT2 PES.

III. RESULTS AND DISCUSSION

A. The potential energy surfaces

In Fig. 3, we present the isotropic components, f^{000}, of the singlet and triplet CC-PT2 and CC-MRCI PESs and compare them with the corresponding terms of the Perugia potential. For completeness, we also show the RCCSD(T) isotropic term for the quintet multiplicity already reported in Ref. 29. First, it can be seen that CC-PT2 and CC-MRCI calculations provide very similar singlet and triplet curves, the CC-PT2 terms being slightly more attractive than the CC-MRCI ones [differences in the well depth are about 0.5 meV (4%) and 0.3 meV (3%) for the singlet and triplet curves, respectively]. Regarding the comparison with the Perugia PES,[16] the largest differences are found for the singlet multiplicity, where the Perugia well depth is about 1.8 meV larger than the CC-PT2 one and the repulsive wall is located at somewhat shorter intermolecular distances. The best agreement is found for the state of largest multiplicity, being particularly remarkable in the repulsive region.[29] It is interesting to note that the splittings between the three spin states are smaller in the *ab initio* than in the experimentally derived PESs. In any case, we consider the comparison between the *ab initio* and the experimentally derived PESs to be quite satisfactory, taking into account the very different procedures used to obtain them.

The anisotropy terms of the Perugia PES, f^{202}, f^{220}, and f^{222}, are compared with the corresponding coefficients of the *ab initio* PESs in Fig. 4 for the case of the triplet multiplicity. It can be seen that except for the f^{222} coefficient, large differences appear between the *ab initio* and the experimentally derived PESs. It must be noted that the Perugia PES was

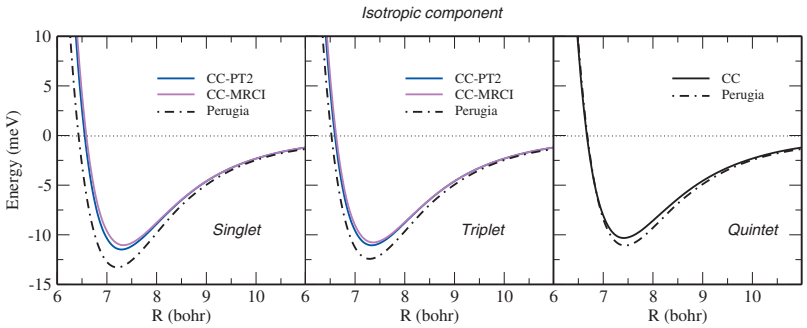

FIG. 3. Isotropic component f^{000} of the singlet, triplet, and quintet PESs compared with the corresponding Perugia terms (Ref. 16). CC-PT2 and CC-MRCI calculations are presented for the singlet and triplet multiplicities, whereas the quintet state corresponds to the RCCSD(T) calculation in Ref. 29. Energies are in meV, and the intermolecular distance is in bohr.

built by including only these three terms to represent the anisotropy of interaction in an effective and compact way[16] (based on the analysis of cross sections measured with rotationally cold beams of aligned molecules as well as on second virial coefficient data). A much larger set of coefficients in the spherical harmonic expansion is involved in the *ab initio* PESs, as detailed below.

In Table II, the complete set of radial coefficients for the singlet surface as well as the triplet-singlet $(t-s)$ splittings for the two types of multiconfigurational calculations are given at an intermolecular distance of 6 bohrs. This distance roughly corresponds to the absolute minimum of the triplet interaction at the rectangular H geometry.[31] It can be seen that, in addition to the f^{000}, f^{202}, f^{220}, and f^{222} coefficients reported in Fig. 4, other terms contribute significantly to the interaction, especially those with $(l_a,l_b,l)=(2\ 2\ 4)$, (4 0 4), (4 2 6), and (4 4 8). This occurs for all the multiplicities and intermolecular distances studied, leading to a globally higher anisotropy for the present PESs with respect to the Perugia ones. It is also interesting to analyze the components of the $t-s$ splittings: the largest splittings are found for the $(l_a,l_b,l)=(0\ 0\ 0)$, (4 4 8), (2 0 2), (2 2 4), and (6 4 10) components of the spherical harmonic expansion. The relevance of the (4 4 8) coefficient in the splittings was already pointed out by Wormer and van der Avoird,[12] and they noted that this is very much related to the nodal character of the partially filled antibonding orbitals π_g of the monomers. On passing, we mention that the relative strength of the radial coefficients shown in Table II is in qualitative agreement with the Hartree–Fock study in Ref. 12 (see Table IV therein). Turning to the comparison between the two types of multiconfigurational calculations, an overall good agreement was found between them, although some quantitative differences (in absolute value) appear for various of the most relevant terms, i.e., $(l_a,l_b,l)=(0\ 0\ 0)$, (4 4 8) and (2 0 2), and this finding is noticed both for the singlet energies as well as for the $t-s$ splittings.

The orientational dependence of the singlet, triplet, and quintet PESs at $R=6$ bohrs is depicted in Fig. 5. Although it has been already pointed out[31] that the multiplet energies do not obey quantitatively the Heisenberg model of the interaction,[11] this model is good enough in order to discuss several features of the figure. Within the Heisenberg Hamiltonian, the singlet, triplet, and quintet PESs can be written as

$$V^s = V_{\rm sa} + 4J,$$

$$V^t = V_{\rm sa} + 2J, \tag{8}$$

$$V^q = V_{\rm sa} - 2J,$$

where $V_{\rm sa}$ is a spin-averaged potential and J is the spin-exchange interaction parameter. In Fig. 5, large (and negative, antiferromagnetic) values of this parameter are found near the rectangular (H) and T-shape geometries, and according to Eq. (8), it can be seen that the quintet-triplet splitting is roughly twice the triplet-singlet one. For some ranges of orientations (between L and H and between T and H), the splittings change sign, the quintet curve becoming slightly more attractive (i.e., the J parameter becoming slightly ferromagnetic). These features agree qualitatively with the Hartree–Fock study of Wormer and van der Avoird[12] (Fig. 1 therein). In addition, as already indicated in Ref. 29, the behavior of the splittings in the path $\mathrm{L}\rightarrow\mathrm{H}\rightarrow\mathrm{X}$ makes the quintet PES exhibit a global minimum at the X geometry (at slightly larger R's) and a local minimum at a planar skewed geometry (at about $\theta_a=\theta_b=71°$ and $R=6.5$ bohrs). Turning to the comparison between the two multiconfigurational approaches, it can be seen that the splittings among the different multiplet states are larger for the CC-PT2 calculation, thus making the CC-PT2 singlet and triplet curves to be more attractive than the corresponding CC-MRCI ones. Although all the terms in Table II contribute (with different weights and signs, depending on the geometry) to the interaction energy, it has been checked that the differences be-

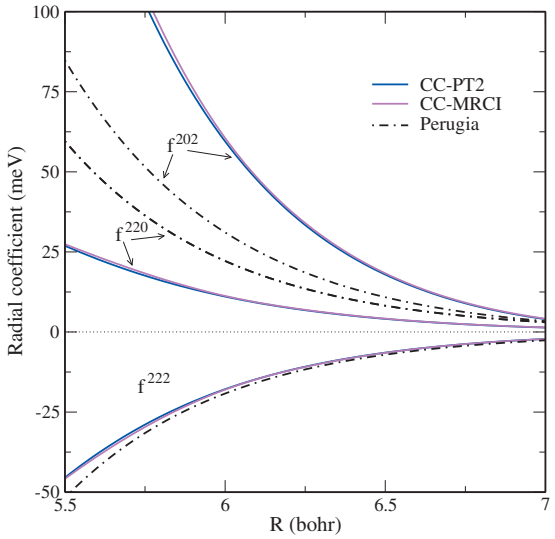

FIG. 4. Anisotropy components f^{202}, f^{220}, and f^{222} of the triplet CC-PT2 and CC-MRCI PESs compared with the Perugia ones (Ref. 16). A similar comparison is found for the singlet multiplicity.

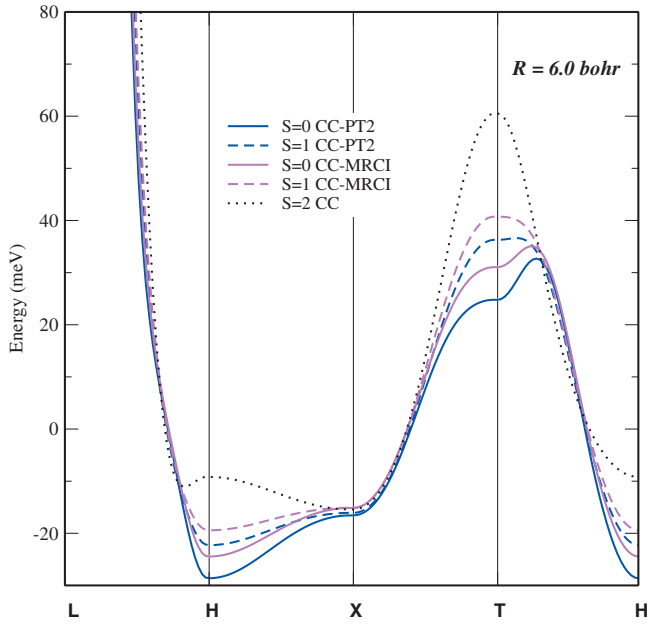

FIG. 5. Orientational dependence at R=6 bohrs of the CC-CASPT2 and CC-MRCI singlet (in solid lines) and triplet (in dashed lines) PESs together with the quintet curve (Ref. 29) [RCCSD(T), black dots]. The geometries change as follows: (a) L→H: $\theta_a=\theta_b=0\rightarrow\pi/2, \phi=0$; (b) H→X: $\theta_a=\theta_b=\pi/2, \phi=0\rightarrow\pi/2$; (c) X→T: $\theta_a=\phi=\pi/2, \theta_b=\pi/2\rightarrow 0$; and (d) T→H: $\theta_a=\pi/2, \phi=0, \theta_b=0\rightarrow\pi/2$. Note that at the L and T geometries, the ϕ torsional angle is undefined.

tween the two multiconfigurational approaches are mainly due to differences in the terms (0 0 0), (2 0 2), and (4 4 8).

B. Integral cross sections

In order to assess the reliability of the *ab initio* PESs, we have tested them against available experimental data such as the total integral cross sections reported in Ref. 16 for the scattering of rotationally hot effusive beams. In these experiments, the oxygen projectile is in a high rotational temperature (with a distribution peaked about levels j=9–13) and collides with the target O_2 molecules, which are in the reaction chamber at low translational temperature. Under these conditions, Aquilanti *et al.* were able to resolve the glory structure, which in turn can give valuable information[46–48] on the intermolecular interaction involved in the process. As has been explained before (see Ref. 16 and references therein), under these experimental conditions, the colliders mainly probe the isotropic component of the interaction, i.e., the anisotropy can be neglected in a first instance. It has been shown, however, that inelastic transitions—due to the anisotropy of the interaction—can eventually modify the details of the glory structure (quenching of the amplitude or location of the extrema).[30,49]

Thus, as a first approximation, we have considered only the spherically averaged interaction given by the first term of the spherical harmonic expansion, f^{000}, for each spin multiplet state, and the cross section calculations have been performed following a Jeffreys-Wentzel-Kramers-Brillouin (JWKB) method. Considering that the total electronic spin S is conserved in the collision, cross sections corresponding to

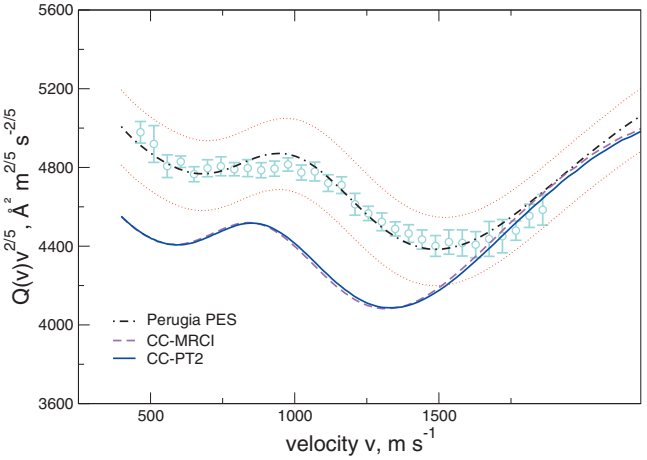

FIG. 6. Total integral cross sections $Q(v)$ times $v^{2/5}$ for scattering of a rotationally hot O_2 effusive beam by O_2 target molecules as functions of the beam velocity, v. Present calculations are in solid and dashed lines as obtained with the CC-PT2 and CC-MRCI PESs, respectively. Experimental data and related best fit calculations (dot-dashed line) are from Ref. 16. Dotted lines refer to the uncertainties in the experimentally derived long range interaction.

the singlet, triplet, and quintet PESs, $Q_s(v)$, $Q_t(v)$, and $Q_q(v)$ respectively, have been combined as follows:

$$Q(v)=\frac{Q_s(v)+3Q_t(v)+5Q_q(v)}{9}, \tag{9}$$

where the weighting factors are determined by degeneracies associated with each spin state and v is the velocity of the molecular beam. More details about the cross section calculation and convolution in the laboratory frame can be found in Ref. 50 and references therein.

In Fig. 6, we report the calculated cross sections computed within the two proposed methodologies (CC-PT2 and CC-MRCI) for the *ab initio* PESs together with the experimental results and those obtained using the Perugia PES.[16] The uncertainty of the experimentally derived C_6^{000} long range term (see Table II of Ref. 16) is shown in the figure by depicting two further dotted lines below and above the best fit dot-dashed one. It can be noticed that both CC-PT2 and CC-MRCI results are very close to each other, given the similar isotropic interactions with the different levels of theory employed (see Fig. 3). It can also be observed that there is an overall reasonable agreement between the *ab initio* and the measured cross sections: the absolute value of our calculations is just few percents lower (<10%) than the experimental best fit, with the glory pattern slightly shifted at lower velocities. This result represents a considerable improvement with respect to that provided by a previous *semi-ab-initio* PES (Ref. 14) (it predicted a glory pattern completely dephased with respect to the experimental one; see Fig. 1 in Ref. 16). It is generally admitted that glory structures of the cross sections provide information on the potential well area,[51,52] while their absolute values contain information about the long range attraction.[53] It must be pointed out that in this context and for the velocities probed experimentally, the "long range region" corresponds to intermolecular distances of about 11–14 bohrs.[30,49]

In view of Figs. 3 and 6, the present results suggest that

TABLE III. Calculated and measured values of the second virial coefficient $B(T)$ ($cm^3\ mol^{-1}$) as a function of temperature (in kelvin). Values corresponding to the contribution given by the spherical component of the interaction are shown in parentheses.

T (K)	Perugia PES[a]	This work CC-MRCI	This work CC-PT2	Experimental Refs. 33 and 34
90	−250 (−211)	−217 (−169)	−223 (−172)	−241 ± 10
100	−204 (−174)	−178 (−138)	−183 (−141)	−197 ± 7
140	−108 (−92)	−94 (−71)	−97 (−73)	−104 ± 5
170	−74 (−62)	−64 (−46)	−66 (−47)	−69 ± 4
210	−47 (−38)	−40 (−26)	−41 (−26)	−45 ± 2
220	−42 (−33)	−35 (−22)	−37 (−23)	−40 ± 2
250	−30 (−23)	−25 (−12.8)	−26 (−13.5)	−29 ± 2
310	−14.1 (−8.5)	−10.5 (−0.6)	−11.4 (−1.2)	−14 ± 1
380	−3.0 (1.7)	−0.4 (8.0)	−1.2 (7.5)	−3 ± 1
400	−0.6 (3.8)	1.7 (9.9)	1.0 (9.4)	−1 ± 1
406	0.0 (4.4)	2.3 (10.4)	1.6 (9.9)	0 ± 1
600	13.1 (16.4)	14.1 (20.6)	13.6 (20.2)	13 ± 1
800	19.1 (21.9)	19.5 (25.1)	19.1 (24.8)	19 ± 1
1000	22.2 (24.7)	22.4 (27.4)	22.0 (27.1)	22.4 ± 1
1400	25.2 (27.3)	25.0 (29.4)	24.7 (29.2)	25.9 ± 1

[a]Reference 16.

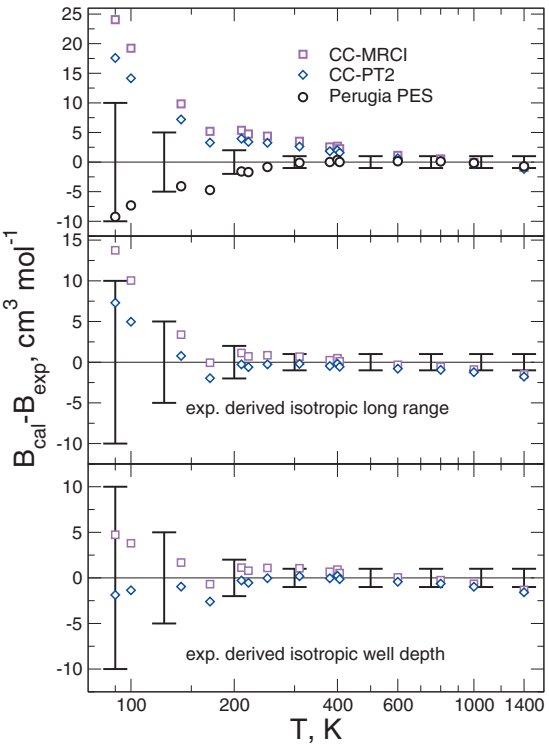

FIG. 7. Deviations between experimental (Refs. 33 and 34) and calculated second virial coefficients $B(T)$. Upper panel: results with present *ab initio* PESs and the Perugia PES (Ref. 16). Intermediate panel: results obtained with present PESs after modification of the long range behavior of the isotropic terms. Lower panel: same as the intermediate panel, but the modification is done on the well depth features of the isotropic terms instead (see text). Abscissas are displayed in log scale for a better resolution at low and intermediates temperatures.

the present *ab initio* PESs could underestimate the isotropic terms, specifically about 1 and 0.1 meV for the well depth and the long range tail (around 13 bohrs), respectively. This conclusion should be taken with caution due to the simplifications of the present dynamical model. For example, by means of close-coupling calculations including the full anisotropy of the quintet PES and at lower velocities,[30] it has been found that the effect of inelastic transitions on the total cross section is a quenching of the glory pattern and a displacement of the extrema toward higher velocities. It would be worthwhile to investigate if more realistic calculations of the nuclear motion improves the comparison with the experiment, and some efforts will be devoted to this issue in the future.

C. Second virial coefficients

A further check on the quality of present PESs—including their anisotropy—can be carried out through the computation of the second virial coefficients $B(T)$ as a function of the temperature T. To calculate this magnitude, we apply a method based on the expressions for two linear molecules presented by Pack,[54] which include the first quantum correction due to the relative translational and rotational motions, including Coriolis coupling. As explained above for the cross sections, partial $B(T)$'s were computed for each multiplet state PES, and the resulting values were properly averaged as in Eq. (9). In Table III and in Fig. 7 (upper panel), the results are compared with the data in Refs. 33 and 34, together with those corresponding to the Perugia PES. In Table III, we also show second virial coefficient calculations performed by just retaining the isotropic component of the PESs under study.

It can be appreciated that both *ab initio* PESs provide a rather good agreement with the experimental data, with small discrepancies at low and intermediate temperatures, which are smaller for the CC-PT2 PESs calculation due to the more attractive character of this potential. The comparison is practically perfect above the Boyle temperature, which indicates that the repulsive walls of our PESs are very well characterized. In more detail, it can be seen that the present *ab initio* and the Perugia PES approximately give lower and upper bounds, respectively, to the measured $B(T)$. The role of the anisotropy can be inferred from the comparison of the full calculation of the $B(T)$'s (including both isotropic and anisotropic components) with the calculation where the anisotropy is neglected (shown in parentheses): the complete $B(T)$'s diminish with respect to the isotropic approximation in a significant manner for all the PESs studied as the temperature decreases. Interestingly, the contribution of the anisotropy is rather more important in the *ab initio* than in the Perugia PESs, as already pointed out in Sec. III A.

From the above discussion, it seems that the present *ab initio* PESs should be slightly more attractive—either in the spherically averaged term or in particular orientations ruled by the anisotropy—in order to achieve a perfect agreement with the measurements. As the results of the previous section (cross sections) indicate that the isotropic terms should be more attractive, we have decided to study the sensitivity of the calculated $B(T)$ to the features of the attractive component of the isotropic interaction. In particular, two different tests have been performed. In the first one, the more attractive long range coefficient C_6^{000} of the Perugia PES (Ref. 16)

has been used to extrapolate (for $R \geq 10$ bohrs) the isotropic terms of the present *ab initio* PESs. In the second analysis, the isotropic term of the *ab initio* quintet PES has been modified to match, in the $6.5 < R < 10$ bohrs range, the corresponding term of the Perugia PES, the isotropic terms of the singlet and triplet PESs being modified as well according to Eq. (1). Results are shown in the central and lower panels of Fig. 7. In both cases, it can be seen that a better agreement with the experimental findings is reached in the lower and intermediate temperature ranges: in the central panel (corresponding to a modification of the long range tail), deviations are within the experimental uncertainties only for the CC-PT2 PES, while an optimal agreement for both *ab initio* PESs is achieved when the modifications are made for the isotropic well depth (lower panel, with the exception of the highest temperature). On the other hand, it can be anticipated that a complete modification of the isotropic terms (both in the well and in the long range regions, as the cross sections results indicate) would bring too low values of the $B(T)$'s.

IV. CONCLUDING REMARKS AND PERSPECTIVES

We have reported new global *ab initio* PESs of the three multiplet spin states for the interaction between rigid oxygen molecules in their ground electronic state. This represents a considerable improvement with respect to previous *ab initio* potentials,[12,14] mainly because now electronic correlation is included by means of high level methods. We expect that this work will be of interest in several fields, such as the absorption of radiation in the atmosphere,[23] thermophysical properties,[55,56] and condensed phase.[57] Our PESs include analytical long range behavior using accurate *ab initio* coefficients,[32] and this characteristic would be particularly useful for studies in cold and ultracold physics.[19,58,59]

The focus of the work has been the calculation of the interaction for the singlet and triplet multiplicities [a quintet RCCSD(T) PESs was previously reported[29]]. Calculations for these lower multiplicities are challenging because the use of multiconfigurational methods is unavoidable, and in this regard, we obtain the singlet and triplet PESs by combining the quintet RCCSD(T) one with MRCI or, alternatively, CASPT2 calculations of the singlet-quintet and triplet-quintet energy splittings.[31]

The resulting two types of PESs, CC-MRCI and CC-PT2, were tested against total cross sections[16] and second virial coefficients[33,34] measurements, and overall, a good agreement has been achieved. The assessment of the anisotropy of the PESs has been crucial in order to compare well with the measured second virial coefficients. It is suggested that an improved agreement with both types of experiments would be achieved if the computed PESs were slightly more attractive. In this sense, the CC-PT2 calculation is relatively more successful, although both types of PESs perform very similarly for the observables here considered. Indeed, these magnitudes do not show high sensitivity to the regions where both types of PESs mostly differ, i.e., the absolute minimum at the rectangular H geometry and the anisotropy of the repulsive wall. High resolution spectra of the dimer[17,18] offer a much more critical test to these surfaces, and calculations of the bound states of the dimer constitute our most immediate work plan.

Further progress in the study of these interactions would be to go beyond the rigid rotor approximation by the incorporation of the dependence of the PESs with the intramolecular (vibrational) degrees of freedom. In the experiments considered here, all molecules must be in their ground vibrational state so that an improved model could consist in obtaining PESs averaged over the ground vibrational state of the monomers. Very recently,[60] vibrational averages of the isotropic (f^{000}) and the leading anisotropic (f^{202}) terms were obtained by means of RCCSD(T) calculations of the quintet state for a set of different intramolecular distances (Gauss–Hermite quadrature points) as well as a reduced set of relative orientations. It was found that the vibrationally averaged terms are just about 1% more attractive (in the well region) than the rigid rotor counterparts while being slightly more repulsive at shorter range. This result suggests that the vibrational dependence of the interaction cannot account for the discrepancies of the present calculations with the experimental data. We rather believe that in addition to future studies using even more accurate *ab initio* methods, improvements of the models for treating the nuclear motions should be addressed, for instance, the inclusion of the anisotropy—and hence, of inelastic transitions—in the calculation of the total cross sections. In addition, new experiments involving less averaged magnitudes should shed some light on the minor uncertainties, which are still beyond reach of current *ab initio* methodologies. As an example, a combined experimental-theoretical study of the evolution of the rotational populations of O_2, measured by Raman spectroscopy along supersonic free jet expansions (as recently done for nitrogen[61]), is in progress.

ACKNOWLEDGMENTS

Financial support by the Ministerio de Ciencia e Innovación (Spain, Grant No. CTQ2007-62898-BQU) is acknowledged. R.H.L. has been supported by a sabbatical grant by the Ministerio de Educación (Spain, Grant No. SAB2009-0010) and by Conacyt (Mexico, Ref. No. 126608).

[1] See the whole volume, *Theoretical and Physical Chemistry*, Encyclopedia of Computational Chemistry Vol. 4, edited by H. F. Schaefer III (Wiley, Chichester, 1998).
[2] X. Li and J. Paldus, J. Chem. Phys. **125**, 164107 (2006).
[3] P. Piecuch, M. Wloch, J. Gour, and A. Kinal, Chem. Phys. Lett. **418**, 467 (2006).
[4] R. Bartlett, Int. J. Mol. Sci. **3**, 579 (2002).
[5] I. Kerkines, P. Carsky, and A. Mavridis, J. Phys. Chem. A **109**, 10148 (2005).
[6] A. Krylov, Annu. Rev. Phys. Chem. **59**, 433 (2008).
[7] D. Zgid and M. Nooijen, J. Chem. Phys. **128**, 144116 (2008).
[8] T. Yanai, Y. Kurashige, E. Neuscamman, and G.-L. Chan, J. Chem. Phys. **132**, 024105 (2010).
[9] S. Das, D. Mukherjee, and M. Kállay, J. Chem. Phys. **132**, 074103 (2010).
[10] G. Chałasiński and M. Szczesniak, Chem. Rev. (Washington, D.C.) **100**, 4227 (2000).
[11] M. van Hemert, P. E. S. Wormer, and A. van der Avoird, Phys. Rev. Lett. **51**, 1167 (1983).
[12] P. E. S. Wormer and A. van der Avoird, J. Chem. Phys. **81**, 1929 (1984).
[13] A. P. J. Jansen and A. van der Avoird, J. Chem. Phys. **86**, 3583 (1987).

[14] B. Bussery and P. E. S. Wormer, J. Chem. Phys. **99**, 1230 (1993).
[15] V. Aquilanti, D. Ascenzi, M. Bartolomei, D. Cappelletti, S. Cavalli, M. de Castro Vitores, and F. Pirani, Phys. Rev. Lett. **82**, 69 (1999).
[16] V. Aquilanti, D. Ascenzi, M. Bartolomei, D. Cappelletti, S. Cavalli, M. de Castro Vitores, and F. Pirani, J. Am. Chem. Soc. **121**, 10794 (1999).
[17] A. Campargue, L. Biennier, A. Kachanov, R. Jost, B. Bussery-Honvault, V. Veyret, S. Churassy, and R. Bacis, Chem. Phys. Lett. **288**, 734 (1998).
[18] L. Biennier, D. Romanini, A. Kachanov, A. Campargue, B. Bussery-Honvault, and R. Bacis, J. Chem. Phys. **112**, 6309 (2000).
[19] B. Friedrich, R. de Carvalho, J. Kim, D. Patterson, J. D. Weinstein, and J. Doyle, J. Chem. Soc., Faraday Trans. **94**, 1783 (1998).
[20] A. V. Avdeenkov and J. L. Bohn, Phys. Rev. A **64**, 052703 (2001).
[21] K. Tilford, M. Hoster, P. M. Florian, and R. C. Forrey, Phys. Rev. A **69**, 052705 (2004).
[22] T. V. Tscherbul, Y. V. Suleimanov, V. Aquilanti, and R. V. Krems, New J. Phys. **11**, 055021 (2009).
[23] A. A. Vigasin and Z. Slanina, *Molecular Complexes in the Earth's, Planetary, Cometary and Interstellar Atmospheres* (World Scientific, Singapore, 1998).
[24] K. Pfeilsticker, H. Bösch, C. Camy-Peyret, R. Fitzenberger, H. Harder, and H. Osterkamp, Geophys. Res. Lett. **28**, 4595 (2001).
[25] D. Perner and U. Platt, Geophys. Res. Lett. **7**, 1053 (1980).
[26] R. Hernández-Lamoneda, M. Bartolomei, M. I. Hernández, J. Campos-Martínez, and F. Dayou, J. Phys. Chem. A **109**, 11587 (2005).
[27] R. Hernández-Lamoneda, M. Bartolomei, E. Carmona-Novillo, M. I. Hernández, J. Campos-Martínez, and F. Dayou, in *Beyond Standard Quantum Chemistry: Applications from Gas to Condensed Phases*, edited by R. Hernández-Lamoneda (Transworld Research Network, Kerala, India, 2007) , ISBN 978-81-7895-293-2.
[28] P. S. Żuchowski, Chem. Phys. Lett. **450**, 203 (2008).
[29] M. Bartolomei, E. Carmona-Novillo, M. I. Hernández, J. Campos-Martínez, and R. Hernández-Lamoneda, J. Chem. Phys. **128**, 214304 (2008).
[30] J. Pérez-Ríos, M. Bartolomei, J. Campos-Martínez, M. I. Hernández, and R. Hernández-Lamoneda, J. Phys. Chem. A **113**, 14952 (2009).
[31] M. Bartolomei, M. I. Hernández, J. Campos-Martínez, E. Carmona-Novillo, and R. Hernández-Lamoneda, Phys. Chem. Chem. Phys. **10**, 5374 (2008).
[32] M. Bartolomei, E. Carmona-Novillo, M. I. Hernández, J. Campos-Martínez, and R. Hernández-Lamoneda, "Long-range interaction for dimers of atmospheric interest: dispersion, induction and electrostatic contributions for O_2–O_2, N_2–N_2 and O_2–N_2," J. Comput. Chem. (2010) (in press).
[33] J. Dymond and E. Smith, *The Virial Coefficient of Pure Gases and Mixtures: a Critical Compilation* (Clarendon, Oxford, 1980).
[34] Dwight E. Gray, *American Institute of Physics Handbook*, 3rd ed. (McGraw-Hill, New York, 1972).
[35] G. S. F. Dhont, J. van Lenthe, G. C. Groenenboom, and A. van der Avoird, J. Chem. Phys. **123**, 184302 (2005).
[36] L. M. C. Janssen, G. C. Groenenboom, A. van der Avoird, P. S. Żuchowski, and R. Podeszwa, J. Chem. Phys. **131**, 224314 (2009).
[37] P. O. Widmark, P. A. Malmqvist, and B. Roos, Theor. Chim. Acta **77**, 291 (1990).
[38] F. M. Tao and Y. K. Pan, J. Chem. Phys. **97**, 4989 (1992).
[39] S. Boys and F. Bernardi, Mol. Phys. **19**, 553 (1970).
[40] J. Van Lenthe, J. van Duijneveldt-Van de Rijdt, and F. Van Duijneveldt, Adv. Chem. Phys. **69**, 521 (1987).
[41] S. R. Langhoff and E. R. Davidson, Int. J. Quantum Chem. **8**, 61 (1974).
[42] E. R. Davidson and D. W. Silver, Chem. Phys. Lett. **52**, 403 (1977).
[43] S. V. J. M. Rintelman, I. Adamovic, and M. S. Gordon, J. Chem. Phys. **122**, 044105 (2005).
[44] M. Heckert, O. Heun, J. Gauss, and P. G. Szalay, J. Chem. Phys. **124**, 124105 (2006).
[45] H.-J. Werner, P. J. Knowles, *et al.*, MOLPRO, version 2002.3, a package of *ab initio* programs (2002); see http://www.molpro.net/.
[46] D. Cappelletti, F. Pirani, B. Bussery-Honvault, L. Gómez, and M. Bartolomei, Phys. Chem. Chem. Phys. **10**, 4281 (2008).
[47] M. Bartolomei, D. Cappelletti, G. de Petris, M. M. Texidor, F. Pirani, M. Rosi, and F. Vecchiocattivi, Phys. Chem. Chem. Phys. **10**, 5993 (2008).
[48] F. Thibault, D. Cappelletti, F. Pirani, and M. Bartolomei, J. Phys. Chem. A **113**, 14867 (2009).
[49] V. Aquilanti, D. Ascenzi, D. Cappelletti, M. de Castro-Vítores, and F. Pirani, J. Chem. Phys. **109**, 3898 (1998).
[50] D. Cappelletti, M. Bartolomei, F. Pirani, and V. Aquilanti, J. Phys. Chem. A **106**, 10764 (2002).
[51] R. B. Bernstein and T. J. P. O'Brien, Discuss. Faraday Soc. **40**, 35 (1965).
[52] R. B. Bernstein and T. J. P. O'Brien, J. Chem. Phys. **46**, 1208 (1967).
[53] F. Pirani and F. Vecchiocattivi, Mol. Phys. **45**, 1003 (1982).
[54] R. T. Pack, J. Chem. Phys. **78**, 7217 (1983).
[55] A. Laesecke, R. Krauss, K. Stephan, and W. Warner, J. Phys. Chem. Ref. Data **19**, 1089 (1990).
[56] M. Abbaspour, E. K. Goharshadi, and J. S. Emampour, Chem. Phys. **326**, 620 (2006).
[57] Y. A. Freiman and H. J. Jodl, Phys. Rep. **401**, 1 (2004).
[58] D. Patterson and J. M. Doyle, J. Chem. Phys. **126**, 154307 (2007).
[59] E. Narevicius, A. Libson, C. G. Parthey, I. Chavez, J. Narevicius, and U. E. M. G. Raizen, Phys. Rev. A **77**, 051401 (2008).
[60] E. Carmona-Novillo, M. Bartolomei, J. Pérez-Ríos, J. Campos-Martínez, and M. I. Hernández, "Diatom-diatom interactions: Building potential energy surfaces and effect of intramolecular vibrations," Int. J. Quantum Chem. (2010) (in press).
[61] J. P. Fonfría, A. Ramos, F. Thibault, G. Tejeda, J. M. Fernández, and S. Montero, J. Chem. Phys. **127**, 134305 (2007).